

Consistent two-lifetime model for spectral functions of superconductors

František Herman and Richard Hlubina

Department of Experimental Physics, Comenius University, Mlynská Dolina F2, 842 48 Bratislava, Slovakia

Recently it has been found that models with at least two lifetimes have to be considered when analyzing the angle resolved photoemission data in the nodal region of the cuprates [T. Kondo et al., Nat. Commun. 6, 7699 (2015)]. In this paper we compare two such models. First we show that the phenomenological model used by Kondo et al. violates the sum rule for the occupation number. Next we consider the recently proposed model of the so-called Dynes superconductors, wherein the two lifetimes measure the strengths of pair-conserving and pair-breaking processes. We demonstrate that the model of the Dynes superconductors is fully consistent with known exact results and we study in detail the resulting spectral functions. Finally, we show that the spectral functions in the nodal region of the cuprates can be fitted well by the model of the Dynes superconductors.

PACS numbers: PACS

I. INTRODUCTION

Recent experimental progress in angle resolved photoemission spectroscopy (ARPES)¹ enables not only to determine the position of features in the electron spectral function, but also to study more subtle issues such as the spectral lineshapes. At least for the conventional low-temperature superconductors, there does exist a theoretical technique which can address such issues - namely the Eliashberg theory,² which allows for strong coupling between the electrons and bosonic collective modes. However, it is not obvious whether this type of theory is applicable to the cuprates. Moreover, even conventional superconductors may possess complicated phonon spectra and/or they can exhibit substantial elastic scattering,³ both of which complicate the Eliashberg analysis. For all these reasons, it is desirable to have a simple and generic theory which does take finite quasiparticle lifetimes in superconductors into account.

Let us start by noting that spectral functions of a BCS superconductor in presence of elastic pair-conserving scattering can be found even in textbooks.^{2,4} However, it is well known that the density of states (or the so-called tomographic density of states in case of anisotropic superconductors⁵) implied by such spectral functions exhibits a full spectral gap consistent with the Anderson theorem. On the other hand, experimentally, the gap is quite often only partial^{3,5} and the tunneling density of states is better described by the phenomenological Dynes formula.^{6,7} This means then that, in order to take the non-trivial density of states into account, also a second type of scattering processes - which are not subject to the Anderson theorem - have to be considered. Two-lifetime phenomenology of precisely this type has in fact been applied quite recently,⁸ with the aim to parameterize the high-resolution ARPES data in the nodal region of the cuprates.

The goals of this paper are twofold. First, in Section 2 we demonstrate that the model used in Ref. 8 can be cast into a form consistent with the generalized Eliashberg theory, and that it exhibits several attractive features. However, we also show that the resulting 2×2 Nambu-

Gor'kov propagator violates the sum rule for the occupation number and therefore the model used in Ref. 8 should be discarded.

Our second goal is to demonstrate that, nevertheless, a fully consistent two-lifetime phenomenology for superconductors does exist. To this end we consider the recently proposed model of the so-called Dynes superconductors,⁹ wherein the two-lifetime phenomenology results as a consequence of taking into account both, the pair-conserving and the pair-breaking scattering processes. In Section 3 we present detailed predictions for the spectral functions of the Dynes superconductors and we explicitly demonstrate the applicability of this approach to the low-temperature ARPES data in the nodal region of the cuprates. Furthermore, in the Appendices we show that the model of the Dynes superconductors is fully consistent with known exact results, and we present explicit formulas for the momentum distribution functions¹⁰ within the Eliashberg theory. Finally, in Section 4 we present our conclusions.

II. THE MODEL USED BY KONDO ET AL.

Following previous theoretical suggestions,^{11,12} the authors of Ref. 8 fit their high resolution ARPES data in the nodal region of optimally doped and overdoped Bi2212 samples to spectral functions derived from the phenomenological self energy

$$\Sigma(\mathbf{k}, \omega) = -i\Gamma_1 + \frac{\bar{\Delta}^2}{\omega + \varepsilon_{\mathbf{k}} + i\Gamma_0} \quad (1)$$

and they interpret the scattering rates Γ_1 and Γ_0 as the single-particle and pair scattering rates, respectively. We shall comment on these identifications later.

In order to demonstrate the physical meaning of the phenomenological self energy Eq. (1), let us first note that it implies that the electron Green function in the superconducting state can be written in the form

$$G(\mathbf{k}, \omega) = \frac{(\omega + i\gamma) + (\varepsilon_{\mathbf{k}} + i\gamma')}{(\omega + i\gamma)^2 - (\varepsilon_{\mathbf{k}} + i\gamma')^2 - \bar{\Delta}^2}, \quad (2)$$

where we have introduced $\gamma = (\Gamma_0 + \Gamma_1)/2$ and $\gamma' = (\Gamma_0 - \Gamma_1)/2$. According to Ref. 8, throughout the superconducting phase $\gamma' < 0$. With increasing temperature $|\gamma'|$ decreases and it vanishes at the critical temperature.

The main observation of this Section is that Eq. (2) should form the upper left component of the general 2×2 Nambu-Gor'kov Green function for a superconductor:

$$\hat{G}(\mathbf{k}, \omega) = \frac{\omega Z(\mathbf{k}, \omega) \tau_0 + [\varepsilon_{\mathbf{k}} + \chi(\mathbf{k}, \omega)] \tau_3 + \phi(\mathbf{k}, \omega) \tau_1}{[\omega Z(\mathbf{k}, \omega)]^2 - [\varepsilon_{\mathbf{k}} + \chi(\mathbf{k}, \omega)]^2 - \phi(\mathbf{k}, \omega)^2}, \quad (3)$$

where τ_i are the Pauli matrices, $Z(\mathbf{k}, \omega)$ is the wavefunction renormalization, and $\phi(\mathbf{k}, \omega)$ is the anomalous self-energy. The function $\chi(\mathbf{k}, \omega)$ describes the renormalization of the single-particle spectrum and it vanishes in a particle-hole symmetric theory; that is why it is usually neglected. For the sake of completeness, let us mention that the matrix τ_2 does not enter Eq. (3), because we work in a gauge with a real order parameter.

Since in the high-frequency limit the functions χ , ϕ , and $\omega(Z - 1)$ should stay at most constant, Eq. (2) in this limit can be uniquely interpreted in terms of the general expression Eq. (3) with

$$Z(\omega) = 1 + i\gamma/\omega, \quad \chi(\omega) = i\gamma', \quad \phi(\omega) = \bar{\Delta}, \quad (4)$$

where we have chosen a real anomalous self-energy ϕ . One checks readily that Eq. (4) reproduces Eq. (2) for all frequencies. The finite value of χ is unusual but seems to be attractive, since the cuprates, being doped Mott insulators, might be expected to break the particle-hole symmetry. Note also that all three functions Z , χ and ϕ do not depend on \mathbf{k} , which is the standard behavior.

It is well known that the 2×2 formalism leads to a redundant description, and therefore the Green function has to satisfy additional constraints. These constraints are most clearly visible in the Matsubara formalism, therefore let us reformulate Eq. (3) on the imaginary axis, allowing explicitly only for frequency-dependent functions $Z_n = Z(i\omega_n)$, $\chi_n = \chi(i\omega_n)$, and $\phi_n = \phi(i\omega_n)$:

$$\hat{G}(\mathbf{k}, \omega_n) = -\frac{i\omega_n Z_n \tau_0 + (\varepsilon_{\mathbf{k}} + \chi_n) \tau_3 + \phi_n \tau_1}{(\omega_n Z_n)^2 + (\varepsilon_{\mathbf{k}} + \chi_n)^2 + \phi_n^2}. \quad (5)$$

Due to the redundancy of the 2×2 formalism, singlet superconductors have to exhibit the following symmetry:

$$G_{22}(\mathbf{k}, \omega_n) = -G_{11}(\mathbf{k}, -\omega_n). \quad (6)$$

Note that the functions Eq. (4) read as $Z_n = 1 + i\gamma/|\omega_n|$, $\chi_n = i\gamma'$, and $\phi_n = \bar{\Delta}$ on the imaginary axis. It is easy to see that when these expressions are plugged in into Eq. (5), the Green function does satisfy Eq. (6).

An additional attractive feature of the phenomenology Eq. (4) is that it leads (also for finite values of γ') to the Dynes formula for the tunneling density of states,

$$N(\omega) = N_0 \text{Re} \left[\frac{\omega + i\gamma}{\sqrt{(\omega + i\gamma)^2 - \bar{\Delta}^2}} \right], \quad (7)$$

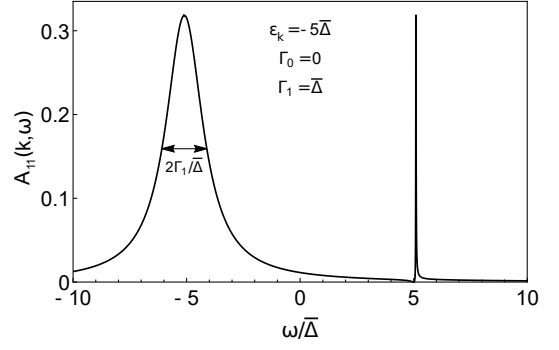


FIG. 1: Spectral function $A_{11}(\mathbf{k}, \omega)$ of an electron inside the Fermi sea according to the model (2). The widths of the electron-like branch at $\omega \approx -E_{\mathbf{k}}$ and of the hole-like branch at $\omega \approx E_{\mathbf{k}}$, where $E_{\mathbf{k}}$ is the quasiparticle energy Eq. (10), are essentially determined by Γ_1 and Γ_0 , respectively.

in agreement with the experimental findings of Ref. 5. The square root has to be taken so that its imaginary part is positive and we keep this convention throughout this paper. In Eq. (7) N_0 denotes the normal-state density of states. Note that, although the particle-hole symmetry is broken due to $\chi \neq 0$, $N(\omega)$ is an even function of ω .

The broken particle-hole symmetry is clearly visible already in the normal state with $\bar{\Delta} = 0$, in which case

$$G_{11}(\mathbf{k}, \omega) = \frac{1}{\omega - \varepsilon_{\mathbf{k}} + i\Gamma_1}, \quad G_{22}(\mathbf{k}, \omega) = \frac{1}{\omega + \varepsilon_{\mathbf{k}} + i\Gamma_0}. \quad (8)$$

These results show that Γ_0 and Γ_1 should not be interpreted as pair and single-particle scattering rates as has been done in Ref. 8, but rather as the scattering rates for the holes and for the electrons, respectively.

Unfortunately, Eqs. (8) turn out to be mutually inconsistent, but in a quite subtle way. In order to show this, let us introduce the spectral functions $A_{ii}(\mathbf{k}, \omega)$ with $i = 1, 2$, corresponding to the Green functions $G_{ii}(\mathbf{k}, \omega)$. Applying standard procedures, the following exact sum rules can be established,

$$\int_{-\infty}^{\infty} \frac{d\omega}{1 + e^{-\omega/T}} A_{11}(\mathbf{k}, \omega) = \langle c_{\mathbf{k}\uparrow} c_{\mathbf{k}\uparrow}^\dagger \rangle = 1 - n_{\mathbf{k}\uparrow},$$

$$\int_{-\infty}^{\infty} \frac{d\omega}{1 + e^{-\omega/T}} A_{22}(\mathbf{k}, \omega) = \langle c_{-\mathbf{k}\downarrow}^\dagger c_{-\mathbf{k}\downarrow} \rangle = n_{-\mathbf{k}\downarrow}.$$

But in a singlet superconductor we have $n_{\mathbf{k}\uparrow} = n_{-\mathbf{k}\downarrow}$, and therefore the following exact relation should hold:

$$\int_{-\infty}^{\infty} \frac{d\omega}{1 + e^{-\omega/T}} [A_{11}(\mathbf{k}, \omega) + A_{22}(\mathbf{k}, \omega)] = 1. \quad (9)$$

Making use of Eqs. (8) at $T = 0$, the integrals on the left-hand side can be taken easily and the results are

$$\int_0^{\infty} d\omega A_{11}(\mathbf{k}, \omega) = \frac{1}{2} + \frac{1}{\pi} \arctan \left(\frac{\varepsilon_{\mathbf{k}}}{\Gamma_1} \right),$$

$$\int_0^{\infty} d\omega A_{22}(\mathbf{k}, \omega) = \frac{1}{2} - \frac{1}{\pi} \arctan \left(\frac{\varepsilon_{\mathbf{k}}}{\Gamma_0} \right).$$

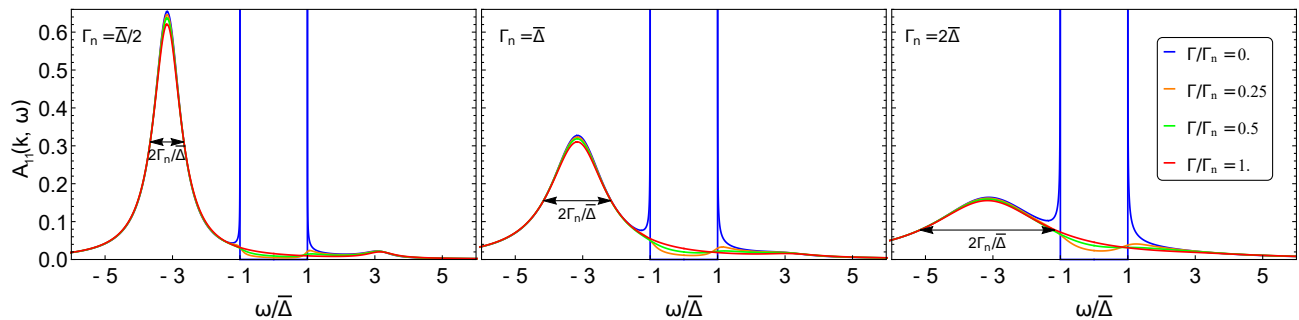


FIG. 2: Spectral functions $A_{11}(\mathbf{k}, \omega)$ of the Dynes superconductor for an electron inside the Fermi sea with $\varepsilon_{\mathbf{k}} = -3\bar{\Delta}$. The total scattering rate $\Gamma_n = \Gamma + \Gamma_s$ increases from the left to the right panel. The curves in each panel differ by the strength of the pair-breaking scattering rate Γ , while Γ_n is kept fixed. The color coding is the same in all panels.

It can be seen readily that, if $\Gamma_0 \neq \Gamma_1$, the sum rule (9) is violated by these results.

One might have the impression that the particle-hole asymmetry which causes the sum rule violation is an artifact of our generalization of the Green function (2) to the matrix form (3). That this is not the case can be seen by plotting the spectral function directly for Eq. (2), see Fig. 1, which clearly shows that the electron- and hole-like branches exhibit different scattering rates.

We conclude that the phenomenology (4) is internally consistent only if $\Gamma_0 = \Gamma_1 = \gamma$, in which case $\gamma' = 0$. But then the Green function (3) has a simple two-pole structure with poles at $\omega = \pm E_{\mathbf{k}} - i\gamma$ where

$$E_{\mathbf{k}} = \sqrt{\varepsilon_{\mathbf{k}}^2 + \bar{\Delta}^2}, \quad (10)$$

implying that the spectral function is a sum of two Lorentzians. However, the authors of Ref. 8 stress that the experimentally observed lineshapes are asymmetric. This means then that the phenomenology (4) is not applicable to the nodal spectral functions of the cuprates.

III. DYNES SUPERCONDUCTORS

Very recently, a consistent two-lifetime phenomenology for superconductors has been derived within the coherent potential approximation, assuming a Lorentzian distribution of pair-breaking fields and an arbitrary distribution of pair-conserving disorder.⁹ If we denote the pair-breaking and pair-conserving scattering rates as Γ and Γ_s , respectively, then the result of Ref. 9 for the Nambu-Gor'kov Green function of the disordered superconductor can be written as

$$\hat{G}(\mathbf{k}, \omega) = \frac{(1 + i\Gamma_s/\Omega) [(\omega + i\Gamma)\tau_0 + \bar{\Delta}\tau_1] + \varepsilon_{\mathbf{k}}\tau_3}{(\Omega + i\Gamma_s)^2 - \varepsilon_{\mathbf{k}}^2}, \quad (11)$$

where

$$\Omega(\omega) = \sqrt{(\omega + i\Gamma)^2 - \bar{\Delta}^2}. \quad (12)$$

Some useful properties of the function $\Omega(\omega)$ are described in Appendix A. The tunneling density of states implied

by the Green function Eq. (11) is described by the Dynes formula Eq. (7) with $\gamma = \Gamma$, and that is why superconductors described by Eq. (11) have been called Dynes superconductors in Ref. 9. In this work we shall keep this term.

It is worth pointing out that in absence of pair-breaking processes, Eq. (11) reproduces the textbook results for pair-conserving scattering, see e.g. Refs. 2,4. On the other hand, in the opposite limit $\Gamma_s = 0$ when only pair-breaking processes are present, Eq. (11) coincides with the phenomenology (4) in the physically consistent case with $\Gamma_0 = \Gamma_1 = \Gamma$. Moreover, in the normal state with $\bar{\Delta} = 0$ the Green function Eq. (11) becomes diagonal and its matrix elements are

$$G_{11}(\mathbf{k}, \omega) = \frac{1}{\omega - \varepsilon_{\mathbf{k}} + i\Gamma_n}, \quad G_{22}(\mathbf{k}, \omega) = \frac{1}{\omega + \varepsilon_{\mathbf{k}} + i\Gamma_n}, \quad (13)$$

where $\Gamma_n = \Gamma + \Gamma_s$ is the total scattering rate, which involves both, pair-breaking as well as pair-conserving scattering processes. Note that Eq. (13) does not exhibit the pathologies implied by Eq. (8).

One checks readily that the Green function Eq. (11) is analytic in the upper half-plane of complex frequencies, as required by causality, and that $\hat{G}(\mathbf{k}, \omega) \propto \tau_0/|\omega|$ for $|\omega| \rightarrow \infty$. In Appendix B, we present an explicit proof that Eq. (11) satisfies the well-known sum rules for the zero-order moments of the electron spectral function, in particular also the sum rule Eq. (9). Moreover, in Appendix D we prove that the electron and hole spectral functions are positive-definite, as required by general considerations.

In view of these observations, we believe that Eq. (11) represents the simplest internally consistent Green function for a superconductor with simultaneously present pair-breaking and pair-conserving scattering processes. This generic BCS-like Green function is parameterized by three energy scales: scattering rates Γ and Γ_s , as well as by the gap parameter $\bar{\Delta}$. In what follows we present a detailed analysis of its spectral properties.

Spectral functions of the Dynes superconductor for an electron with momentum \mathbf{k} fixed to lie inside the Fermi sea are shown in Fig. 2. The BCS quasiparticle peaks at

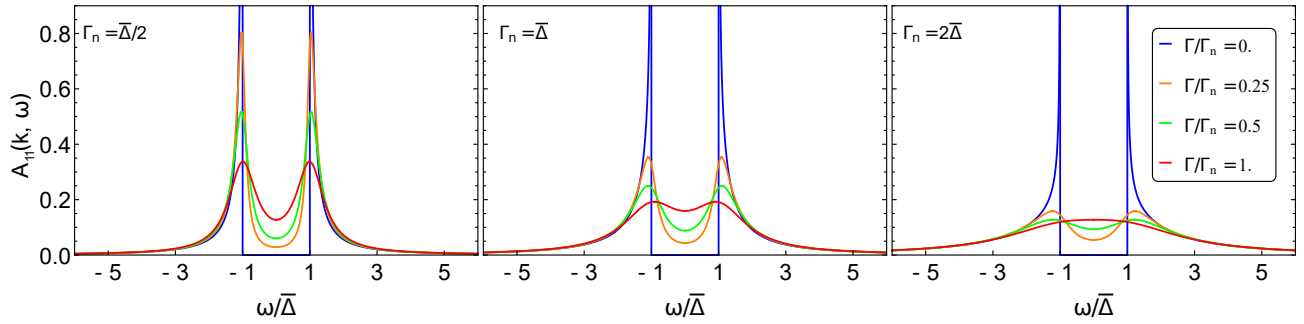


FIG. 3: Spectral functions $A_{11}(\mathbf{k}, \omega)$ of the Dynes superconductor for an electron directly at the Fermi surface, $\varepsilon_{\mathbf{k}} = 0$. The total scattering rate $\Gamma_n = \Gamma + \Gamma_s$ increases from the left to the right panel. The curves in each panel differ by the strength of the pair-breaking scattering rate Γ , while Γ_n is kept fixed. The color coding is the same in all panels.

$\omega \approx \pm E_{\mathbf{k}}$ are seen to be broadened by the total scattering rate Γ_n , irrespective of the ratio between pair-breaking and pair-conserving scattering processes. The relative importance of the two types of processes becomes important only in the vicinity of the chemical potential. For $\Gamma = 0$ a full spectral gap appears for $|\omega| < \bar{\Delta}$, in agreement with the Anderson theorem, and additional peaks appear in the spectral function at $\omega = \pm \bar{\Delta}$. After switching on a finite pair breaking rate $\Gamma \neq 0$, the spectral gap starts to fill in, and at the same time the peaks at $\omega = \pm \bar{\Delta}$ get smeared away. Finally, when $\Gamma = \Gamma_n$ and the pair-conserving processes disappear completely, the spectral function is given by a sum of two Lorentzians centered at $\omega = \pm E_{\mathbf{k}}$.

Spectral functions for an electron directly at the Fermi surface, $\varepsilon_{\mathbf{k}} = 0$, are somewhat different and they are shown in Fig. 3. The difference is caused by the fact that the quasiparticle energies $\pm E_{\mathbf{k}}$ in this case coincide with $\pm \bar{\Delta}$. Therefore only two peaks are present in the spectral function, in contrast to the general case with four peaks. However, the rest of the phenomenology can be simply related to the case $\varepsilon_{\mathbf{k}} \neq 0$: the high-energy form of the spectral functions is controlled exclusively by the total scattering rate Γ_n , whereas finite pair-breaking fills in the spectral gap and smears the peaks at $\omega = \pm \bar{\Delta}$.

In Appendix C we complement the discussion of electron spectral functions by studying the so-called momentum distribution functions.¹⁰ In addition to presenting explicit formulas valid for any Eliashberg-type superconductor with only frequency-dependent functions $Z(\omega)$ and $\phi(\omega)$, we also show that making use of the momentum distribution functions, one can determine the total scattering rate Γ_n of a Dynes superconductor in an alternative way.

In Fig. 4 we demonstrate that Eq. (11) can fit the experimentally observed symmetrized spectral functions in the nodal region of the cuprates with at least comparable quality as Eq. (1). The number of fitting parameters is the same for both fits: two scattering rates, the gap $\bar{\Delta}$, and the energy scale Λ which determines the phenomenological background $|\omega|/\Lambda^2$. This type of background description has been used in all fits presented in

Ref. 8. We have determined the fitting parameters by the standard least-squares technique in the interval from -100 meV to 100 meV; their values are $\bar{\Delta} = 25$ meV, $\Gamma = 3.7$ meV, $\Gamma_s = 16$ meV, and $\Lambda = 103$ meV for the fit using Eq. (11). On the other hand, we have found $\bar{\Delta} = 27$ meV, $\Gamma_0 = 0$ meV, $\Gamma_1 = 12$ meV, and $\Lambda = 87$ meV for the fit using Eq. (1).

Both fits find roughly the same value of the gap $\bar{\Delta}$ and of the background parameter Λ , but the scattering rates turn out to be quite different. In view of the latter observation it seems to be worthwhile to repeat the analysis of Ref. 8, but with the ansatz Eq. (11) for the electron Green function. It remains to be seen whether this type of analysis can be applied also at temperatures above T_c , and what is the resulting temperature dependence of the scattering rates Γ and Γ_s .

The small value of the pair-breaking rate Γ with respect to the large pair-conserving rate Γ_s implied by Fig. 4 is consistent with the observation that the concept of the tomographic density of states is useful in the analysis of the ARPES data.^{5,13} Since in an anisotropic superconductor large-angle scattering is pair-breaking, the smallness of Γ implies that the dominant scattering processes (at least in the nodal region and at low temperatures) have to be of the forward-scattering type.

The importance of forward-scattering processes in the nodal region has been confirmed recently also by an analysis of the momentum distribution curves.¹⁴ As for the microscopic origin of the forward scattering, it has been argued that it can be caused by elastic scattering on disorder located outside the CuO_2 planes.¹⁵ Other explanations include scattering on (quasi) static long-range fluctuations, perhaps due to competing order, or scattering on low-energy long-wavelength emergent gauge fields.¹⁶ These different scenarios can be distinguished by different dependence on temperature and/or Fermi-surface location and further experimental work is needed to discriminate between them.

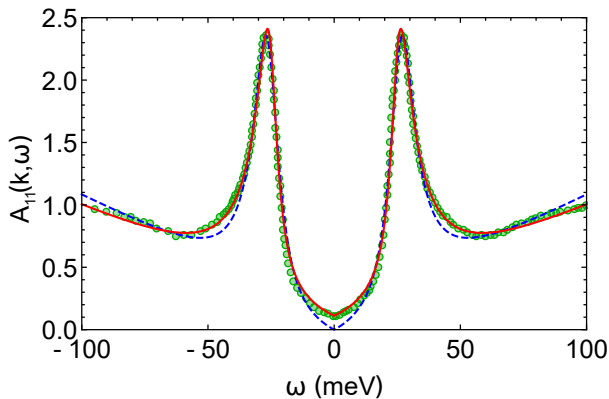


FIG. 4: Experimentally observed low-temperature symmetrized spectral functions at the Fermi level reported in Ref. 8 for optimally doped Bi2212 at angle $\phi = 24^\circ$. Also shown are least-square fits in the region from -100 meV to +100 meV around the Fermi level which make use of Eq. (11) (red solid line) and of Eq. (1) (blue dashed line). The values of the fitting parameters are shown in the main text.

IV. CONCLUSIONS

To summarize, we have shown that the phenomenological self-energy Eq. (1), which has been proposed theoretically in Refs. 11,12 and applied recently in Ref. 8, is internally consistent only in the case when $\Gamma_0 = \Gamma_1$; in this case the electron spectral function in the superconducting state is a sum of two Lorentzians.

The simplest consistent genuine two-lifetime Green function of a superconductor is given by Eq. (11). This model depends on two scattering rates: the pair-breaking scattering rate Γ and the pair-conserving scattering rate Γ_s . The Green function Eq. (11) implies that the density of states is described by the Dynes formula Eq. (7) with $\gamma = \Gamma$ and the electron spectral functions exhibit more structure than might be expected naively, see Figs. 2,3.

The Green function Eq. (11) is analytic in the upper half-plane, it has the correct large-frequency asymptotics, its diagonal spectral functions are positive-definite, and it satisfies the exact sum rules Eq. (9) and Eq. (B3). Moreover, in the three limiting cases of either $\Gamma = 0$, or $\Gamma_s = 0$, or $\bar{\Delta} = 0$, it reduces to the well-known results. Therefore, although Eq. (11) has been originally derived only for a special distribution of pair-breaking fields within the coherent potential approximation, we believe that it represents a *generic* two-lifetime Green function of a superconductor.

Our results provide a (in principle) straightforward recipe for extracting the scattering rates Γ and $\Gamma_n = \Gamma + \Gamma_s$ from experimental data: the pair-breaking scattering rate Γ is best determined from the tunneling (or, in anisotropic superconductors, tomographic⁵) density of states, whereas the total scattering rate Γ_n may be extracted from the widths of the quasiparticle peaks in spectral functions, see Fig. 2. Alternatively, as shown

in Appendix C, the scattering rate Γ_n can be determined from the width of the momentum distribution functions, and it enters also the analysis of optical conductivity.¹⁷

Obviously, description of superconductors making use of Eq. (11) can be quantitatively correct only at energies smaller than the typical boson energies of the studied system. At higher energies, application of a full-fledged Eliashberg-type theory² - but extended so as to allow for processes leading to Eq. (11) at low energies - is unavoidable. For completeness, in Appendix C we have described a procedure which, starting from the assumption of only frequency-dependent Eliashberg functions $Z(\omega)$ and $\Delta(\omega)$, allows for their complete determination from ARPES data by combining two approaches: the momentum distribution technique and the tomographic density of states.

Finally, in Fig. 4 we have demonstrated that the low-temperature ARPES data in the nodal region of the cuprates can be fitted well using Eq. (11). Our results confirm previous claims about the importance of forward-scattering processes in this region, but identification of their physical origin will require further detailed angle- and temperature-dependent studies.

Appendix A: Properties of the function $\Omega(\omega)$

Let us decompose the function $\Omega(\omega)$ defined by Eq. (12) into its real and imaginary parts, $\Omega = \Omega_1 + i\Omega_2$. One finds readily that $\Omega_{1,2}$ should satisfy the relations

$$\Omega_1\Omega_2 = \omega\Gamma, \quad \Omega_1^2 - \Omega_2^2 = \nu^2, \quad (\text{A1})$$

where $\nu^2 = \omega^2 - \bar{\Delta}^2 - \Gamma^2$. Our sign convention leads then to the following explicit expressions for $\Omega_{1,2}$:

$$\begin{aligned} \Omega_1(\omega) &= \text{sgn}(\omega) \sqrt{\left[\sqrt{\nu^4 + 4\omega^2\Gamma^2} + \nu^2 \right] / 2}, \\ \Omega_2(\omega) &= \sqrt{\left[\sqrt{\nu^4 + 4\omega^2\Gamma^2} - \nu^2 \right] / 2}. \end{aligned}$$

Note that $\Omega_1(\omega)$ is an odd function of ω , while $\Omega_2(\omega)$ is positive definite and even. A straightforward calculation shows that for $\omega > 0$ the following inequalities are valid:

$$\Omega_1 \leq \omega, \quad \Omega_2 \geq \Gamma. \quad (\text{A2})$$

These inequalities will be used in Appendix D.

It is worth pointing out that the function $\Omega_1(\omega)$ characterizing the Dynes superconductor is in principle directly measurable in low-temperature tunneling experiments. In fact, it is well known that in such experiments the derivative of the current-voltage characteristics, dI/dV , is proportional to the tunneling density of states $N(\omega)$ with $\omega = eV$. But, since $N(\omega) \propto d\Omega_1/d\omega$, the function $\Omega_1(\omega)$ is proportional to the measured function $I = I(V)$.

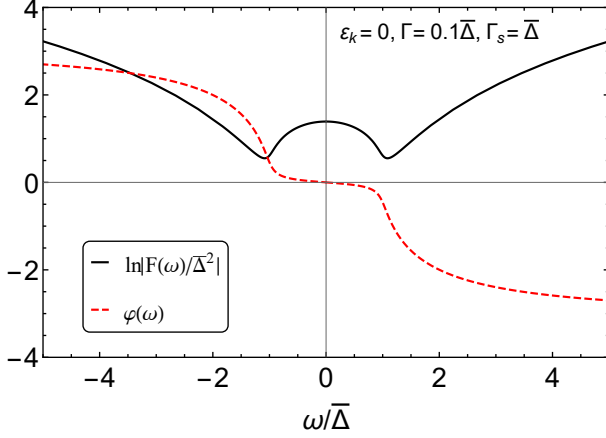


FIG. 5: Real and imaginary parts of the function $H(\omega)$.

Appendix B: Sum rules for the Dynes superconductors

In this Appendix we prove that Eq. (11) satisfies the sum rules for the zero-order moments of the electron spectral function. To this end, let us introduce an auxiliary complex function $F(\omega)$ of the real frequency ω ,

$$F(\omega) = \varepsilon_{\mathbf{k}}^2 - [\Omega(\omega) + i\Gamma_s]^2.$$

Note that the function $F(\omega)$ depends also on the momentum \mathbf{k} , but for the sake of simplicity this dependence will not be displayed explicitly.

Let us furthermore define the function

$$H(\omega) = \ln F(\omega) = \ln |F(\omega)| + i\varphi(\omega).$$

In the second equality we have represented the complex function $F(\omega) = |F(\omega)| \exp\{i\varphi(\omega)\}$ in terms of its amplitude $|F(\omega)|$ and phase $\varphi(\omega)$ constrained to the interval $(-\pi, \pi)$. A plot of the real and imaginary parts of the function $H(\omega)$ is shown in Fig. 5. Note that the phase $\varphi(\omega)$ is an odd function of frequency and its asymptotic values are $\varphi(\pm\infty) = \mp\pi$.

Making use of the function $H(\omega)$, the Nambu-Gor'kov Green function (11) can be written in the following elegant form:

$$\hat{G}(\mathbf{k}, \omega) = \frac{1}{2} \left[\frac{\partial H}{\partial \omega} \tau_0 - \frac{\partial H}{\partial \Delta} \tau_1 - \frac{\partial H}{\partial \varepsilon_{\mathbf{k}}} \tau_3 \right]. \quad (\text{B1})$$

From here follows the following explicit expression for the Nambu-Gor'kov spectral function, defined as usual by $\hat{A}(\mathbf{k}, \omega) = -\pi^{-1} \text{Im} \hat{G}(\mathbf{k}, \omega)$:

$$\hat{A}(\mathbf{k}, \omega) = \frac{1}{2\pi} \left[-\frac{\partial \varphi}{\partial \omega} \tau_0 + \frac{\partial \varphi}{\partial \Delta} \tau_1 + \frac{\partial \varphi}{\partial \varepsilon_{\mathbf{k}}} \tau_3 \right]. \quad (\text{B2})$$

Equation (B2) forms the starting point of our discussion of the sum rules.

Using the oddness of the function $\varphi(\omega)$ and of its asymptotic values, one finds readily that Eq. (B2) implies the matrix equation

$$\int_{-\infty}^{\infty} d\omega \hat{A}(\mathbf{k}, \omega) = \tau_0, \quad (\text{B3})$$

in perfect agreement with the well-known exact sum rule for the zero-order moment of the spectral function.

Next we prove that Eq. (B2) satisfies the exact sum rule Eq. (9). Since $\text{Tr} \hat{A}(\mathbf{k}, \omega) = -\pi^{-1} \partial \varphi / \partial \omega$, we have to prove that

$$\int_{-\infty}^{\infty} \frac{d\omega}{1 + e^{-\omega/T}} \frac{\partial \varphi}{\partial \omega} = -\pi.$$

By calculating the integral on the left-hand side by parts, our task reduces to proving the equality

$$\int_{-\infty}^{\infty} \frac{d\omega}{4T \cosh^2(\omega/2T)} \varphi(\omega) = 0.$$

But, since $\varphi(\omega)$ is odd, this last equality is trivially satisfied. Thus we have proven that the Dynes superconductors satisfy Eq. (9).

For the sake of completeness, let us note that the full matrix form of the sum rule Eq. (9) reads

$$\int_{-\infty}^{\infty} \frac{d\omega}{1 + e^{-\omega/T}} \hat{A}(\mathbf{k}, \omega) = \begin{pmatrix} 1 - n_{\mathbf{k}} & b_{\mathbf{k}} \\ b_{\mathbf{k}} & n_{\mathbf{k}} \end{pmatrix}, \quad (\text{B4})$$

where $n_{\mathbf{k}} = n_{\mathbf{k}\uparrow} = n_{-\mathbf{k}\downarrow}$, $b_{\mathbf{k}} = \langle c_{\mathbf{k}\uparrow} c_{-\mathbf{k}\downarrow} \rangle = \langle c_{-\mathbf{k}\downarrow}^\dagger c_{\mathbf{k}\uparrow}^\dagger \rangle$, and the thermodynamic expectation values $n_{\mathbf{k}}$ and $b_{\mathbf{k}}$ are given by

$$n_{\mathbf{k}} = \frac{1}{2} - \int_0^\infty \frac{d\omega}{2\pi} \frac{\partial \varphi}{\partial \varepsilon_{\mathbf{k}}} \tanh \frac{\omega}{2T},$$

$$b_{\mathbf{k}} = \int_0^\infty \frac{d\omega}{2\pi} \frac{\partial \varphi}{\partial \Delta} \tanh \frac{\omega}{2T}.$$

It should be pointed out that sum rules for higher-order moments of the spectral function which generalize Eqs. (B3, B4) can be also derived, but their right-hand sides depend on the Hamiltonian of the problem. Such sum rules therefore do not provide useful checks of the phenomenological Green function Eq. (11).

Appendix C: Momentum distribution functions in the Eliashberg theory

We have already noted that, within the Eliashberg theory, the functions $Z(\omega)$ and $\phi(\omega)$ usually depend only on frequency ω and are independent of the momentum \mathbf{k} . Quite some time ago, it has been pointed out that in such cases it is useful to study the spectral function $A_{11}(\mathbf{k}, \omega)$ for fixed frequency ω as a function of the bare electron energy $\varepsilon_{\mathbf{k}}$, the so-called momentum distribution function.¹⁰ To simplify the formulas, in this Appendix we will replace $A_{11}(\mathbf{k}, \omega)$ by $A(\varepsilon, \omega)$.

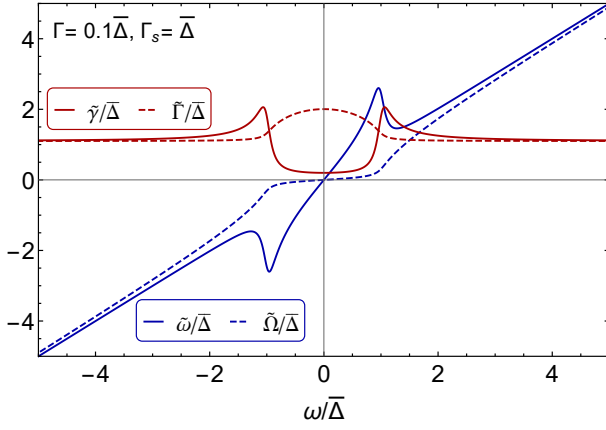


FIG. 6: Functions $\tilde{\omega}(\omega)$, $\tilde{\gamma}(\omega)$, $\tilde{\Omega}(\omega)$, and $\tilde{\Gamma}(\omega)$ for a Dynes superconductor.

Instead of the two complex functions $Z(\omega)$ and $\phi(\omega)$, let us introduce the following four real functions of frequency $\tilde{\omega}(\omega)$, $\tilde{\gamma}(\omega)$, $\tilde{\Omega}(\omega)$, and $\tilde{\Gamma}(\omega)$:

$$\begin{aligned} \omega Z &= \tilde{\omega} + i\tilde{\gamma}, \\ \sqrt{(\omega Z)^2 - \phi^2} &= \tilde{\Omega} + i\tilde{\Gamma}. \end{aligned} \quad (C1)$$

To illustrate their symmetries and typical form, in Fig. 6 we plot the functions $\tilde{\omega}(\omega)$, $\tilde{\gamma}(\omega)$, $\tilde{\Omega}(\omega)$, and $\tilde{\Gamma}(\omega)$ for a Dynes superconductor.

After a tedious but straightforward calculation the spectral function of a general Eliashberg superconductor can be written as

$$\begin{aligned} A(\varepsilon, \omega) &= \frac{1}{2} \left[\frac{\tilde{\gamma}}{\tilde{\Gamma}} + 1 \right] \delta_{\tilde{\Gamma}}(\varepsilon - \tilde{\Omega}) + \frac{1}{2} \left[\frac{\tilde{\gamma}}{\tilde{\Gamma}} - 1 \right] \delta_{\tilde{\Gamma}}(\varepsilon + \tilde{\Omega}) \\ &+ \frac{1}{2} \left[\frac{\tilde{\omega}}{\tilde{\Omega}} - \frac{\tilde{\gamma}}{\tilde{\Gamma}} \right] \frac{4\pi\tilde{\Omega}^2}{\tilde{\Gamma}} \delta_{\tilde{\Gamma}}(\varepsilon - \tilde{\Omega}) \delta_{\tilde{\Gamma}}(\varepsilon + \tilde{\Omega}), \end{aligned} \quad (C2)$$

where we have introduced the notation

$$\delta_{\tilde{\Gamma}}(x) = \frac{1}{\pi} \frac{\tilde{\Gamma}}{x^2 + \tilde{\Gamma}^2}$$

for a Lorentzian with width $\tilde{\Gamma}$. According to Eq. (C2), the spectral function $A(\varepsilon, \omega)$, when viewed as a function of energy ε at fixed frequency ω , consists of three terms. The first two terms are Lorentzians, whereas the third term is a product of two Lorentzians.

When the measured momentum distribution functions are fitted by Eq. (C2), $\tilde{\Omega}$ can be determined from the positions of the Lorentzians and $\tilde{\Gamma}$ is given by their widths. Finally, from the relative weights of the three terms in Eq. (C2) one can determine the ratios $\tilde{\gamma}/\tilde{\Gamma}$ and $\tilde{\omega}/\tilde{\Omega}$. With all four functions $\tilde{\omega}(\omega)$, $\tilde{\gamma}(\omega)$, $\tilde{\Omega}(\omega)$, and $\tilde{\Gamma}(\omega)$ known, one obtains full information about the superconducting state. This idea has been used in an impressive set of recent papers, see Ref.18 and references therein.

One should note, however, that in order to determine all four parameters $\tilde{\omega}$, $\tilde{\gamma}$, $\tilde{\Omega}$, and $\tilde{\Gamma}$, it is necessary to

resolve all three terms in Eq. (C2), together with their relative weights. But at sufficiently large frequencies we should expect that $\tilde{\Gamma} \ll |\tilde{\Omega}|$, see Fig. 6. In this case the following approximate equality is valid

$$\frac{4\pi\tilde{\Omega}^2}{\tilde{\Gamma}} \delta_{\tilde{\Gamma}}(\varepsilon - \tilde{\Omega}) \delta_{\tilde{\Gamma}}(\varepsilon + \tilde{\Omega}) \approx \delta_{\tilde{\Gamma}}(\varepsilon - \tilde{\Omega}) + \delta_{\tilde{\Gamma}}(\varepsilon + \tilde{\Omega}),$$

which means that the product of two Lorentzians can not be distinguished from their sum. Inserting this equality into Eq. (C2), one finds readily that the spectral function $A(\varepsilon, \omega)$ is given by a sum of only two Lorentzians,

$$A(\varepsilon, \omega) \approx \frac{1}{2} \left[\frac{\tilde{\omega}}{\tilde{\Omega}} + 1 \right] \delta_{\tilde{\Gamma}}(\varepsilon - \tilde{\Omega}) + \frac{1}{2} \left[\frac{\tilde{\omega}}{\tilde{\Omega}} - 1 \right] \delta_{\tilde{\Gamma}}(\varepsilon + \tilde{\Omega}).$$

But if this is the case, then from fits to the momentum distribution function one can determine only $\tilde{\Omega}$, $\tilde{\Gamma}$, and $\tilde{\omega}$, but not $\tilde{\gamma}$. In other words, we do not have access to the pairing function $\phi^2(\omega) = (\tilde{\omega} + i\tilde{\gamma})^2 - (\tilde{\Omega} + i\tilde{\Gamma})^2$ in this frequency limit.

There is yet another reason why fits to the momentum distribution function can provide reliable estimates of the Eliashberg parameters only for $|\omega| \lesssim \bar{\Delta}$: namely, this technique requires that both ratios, $\tilde{\gamma}/\tilde{\Gamma}$ and $\tilde{\omega}/\tilde{\Omega}$, are sufficiently different from 1, so that the weights of the second and third terms in Eq. (C2) can be determined precisely. But Fig. 6 clearly shows that this criterion is satisfied only for $|\omega| \lesssim \bar{\Delta}$.

Does this mean that the Eliashberg problem of finding the functions $Z(\omega)$ and $\Delta(\omega)$ can not be solved in the frequency range $\bar{\Delta} \lesssim |\omega|$? The answer is no: it has been pointed out recently^{18,19} that, by applying the powerful inversion technique developed in Ref. 20, it is possible to extract the complex gap function $\Delta(\omega) = \phi(\omega)/Z(\omega)$ from the measured tomographic density of states. When this knowledge is combined with the momentum distribution technique - which allows for a relatively straightforward determination of $\tilde{\Omega}$ and $\tilde{\Gamma}$ in the limit $\bar{\Delta} \lesssim |\omega|$ with one Lorentzian only - making use of the expression

$$Z(\omega) = \frac{\tilde{\Omega} + i\tilde{\Gamma}}{\sqrt{\omega^2 - \Delta^2(\omega)}}$$

one can determine also the second Eliashberg function $Z(\omega)$, thereby solving the Eliashberg problem.¹⁸

Finally, let us note that the momentum distribution functions can be useful also in the special case of the Dynes superconductors described by Eq. (11). In fact, since in the frequency range $\bar{\Delta} \lesssim |\omega|$ the width of the observable Lorentzian in the momentum distribution function of a Dynes superconductor is $\tilde{\Gamma} \approx \Gamma_n$, this gives us an independent procedure for measuring the total scattering rate $\Gamma_n = \Gamma + \Gamma_s$.

Appendix D: Proof of the inequalities $A_{ii}(\mathbf{k}, \omega) \geq 0$ for the Dynes superconductors

In this Appendix we will prove that the diagonal spectral functions $A_{ii}(\mathbf{k}, \omega)$ of the Dynes superconductors are positive-definite, as required by general considerations.

To this end, let us first note that the diagonal components of the Nambu-Gor'kov Green function within the Eliashberg theory read as

$$G_{ii}(\mathbf{k}, \omega) = \frac{\tilde{\omega} + i\tilde{\gamma} \pm \varepsilon_{\mathbf{k}}}{(\tilde{\Omega} + i\tilde{\Gamma})^2 - \varepsilon_{\mathbf{k}}^2}.$$

Since $A_{ii}(\mathbf{k}, \omega) = -\pi^{-1} \text{Im} G_{ii}(\mathbf{k}, \omega)$, from here it follows that the requirement $A_{ii}(\mathbf{k}, \omega) \geq 0$ is equivalent to

$$2\tilde{\Omega}\tilde{\Gamma}\tilde{\omega} - \tilde{\gamma}(\tilde{\Omega}^2 - \tilde{\Gamma}^2) \geq -\tilde{\gamma}\varepsilon_{\mathbf{k}}^2 \mp 2\tilde{\Omega}\tilde{\Gamma}\varepsilon_{\mathbf{k}},$$

which has to hold for all $\varepsilon_{\mathbf{k}}$ and ω . Maximizing the expression on the right-hand side with respect to $\varepsilon_{\mathbf{k}}$, this requirement can be rewritten as

$$\frac{\tilde{\gamma}^2\tilde{\Gamma}^2}{\tilde{\gamma}^2 + \tilde{\Gamma}^2} + \tilde{\omega}\tilde{\Omega}\frac{2\tilde{\gamma}\tilde{\Gamma}}{\tilde{\gamma}^2 + \tilde{\Gamma}^2} \geq \tilde{\Omega}^2,$$

which has to be valid for all frequencies ω . Since the first term on the left-hand side is obviously positive, it follows that it is sufficient to show that

$$\frac{\tilde{\omega}}{\tilde{\Omega}} \geq \frac{1}{2} \left(\frac{\tilde{\gamma}}{\tilde{\Gamma}} + \frac{\tilde{\Gamma}}{\tilde{\gamma}} \right).$$

In order to prove this latter inequality, we will prove the following two simpler inequalities:

$$\frac{\tilde{\omega}}{\tilde{\Omega}} \geq \frac{\tilde{\gamma}}{\tilde{\Gamma}}, \quad \frac{\tilde{\omega}}{\tilde{\Omega}} \geq \frac{\tilde{\Gamma}}{\tilde{\gamma}}. \quad (\text{D1})$$

In view of the symmetries illustrated by Fig. 6, one checks easily that it is sufficient to prove that these inequalities hold for $\omega > 0$.

So far, our discussion was valid for any Eliashberg superconductor. Now we specialize to the Dynes superconductors. Making use of Eqs. (C1),(11) one finds easily that in this case the quantities $\tilde{\omega}$, $\tilde{\Omega}$, $\tilde{\Gamma}$, and $\tilde{\gamma}$ can be written in terms of the functions Ω_1 and Ω_2 introduced in Appendix A as

$$\begin{aligned} \tilde{\Omega} &= \Omega_1, \\ \tilde{\Gamma} &= \Omega_2 + \Gamma_s, \\ \tilde{\omega} &= \omega + \Gamma_s \frac{\omega\Omega_2 - \Gamma\Omega_1}{\Omega_1^2 + \Omega_2^2}, \\ \tilde{\gamma} &= \Gamma + \Gamma_s \frac{\omega\Omega_1 + \Gamma\Omega_2}{\Omega_1^2 + \Omega_2^2}. \end{aligned}$$

Let us note in passing that these expressions justify the results plotted in Fig. 6.

Next we plug the expressions for $\tilde{\omega}$, $\tilde{\Omega}$, $\tilde{\Gamma}$, and $\tilde{\gamma}$ into Eqs. (D1). If one makes use of the equalities Eqs. (A1) and of the inequalities Eqs. (A2), after some straightforward algebra one can check that the inequalities Eqs. (D1) are satisfied. This completes the proof that, for the Dynes superconductors, the inequalities $A_{ii}(\mathbf{k}, \omega) \geq 0$ are valid.

Acknowledgments

This work was supported by the Slovak Research and Development Agency under contracts No. APVV-0605-14 and No. APVV-15-0496, and by the Agency VEGA under contract No. 1/0904/15.

-
- ¹ M. Hashimoto et al., Nat. Phys. **10**, 483 (2014).
² F. Marsiglio and J. P. Carbotte, in *Superconductivity*, K. H. Bennemann and J. B. Ketterson, Eds., Vol. I, Springer, Berlin, 2008, p. 73.
³ P. Szabó et al., Phys. Rev. B **93**, 014505 (2016).
⁴ L. Zhu, P. J. Hirschfeld, and D. J. Scalapino, Phys. Rev. B **70**, 214503 (2004).
⁵ T. J. Reber et al., Nat. Phys. **8**, 606 (2012).
⁶ R. C. Dynes, V. Narayanamurti, and J. P. Garno, Phys. Rev. Lett. **41**, 1509 (1978).
⁷ A. E. White, R. C. Dynes, and J. P. Garno, Phys. Rev. B **33**, 3549(R) (1986).
⁸ T. Kondo et al., Nat. Commun. **6**, 7699 (2015).
⁹ F. Herman and R. Hlubina, Phys. Rev. B **94**, 144508 (2016).
¹⁰ J.C. Campuzano, M.R. Norman and M. Randeria, *Photoemission in the High Tc Superconductors*, in *The Physics*

- of Superconductors*, K.H. Bennemann and J.B. Ketterson, eds., Vol. II, Springer, New York, 2004, pp. 167-273.
¹¹ M. R. Norman et al., Phys. Rev. B **57**, R11093 (1998).
¹² A. V. Chubukov et al., Phys. Rev. B **76**, 180501 (2007).
¹³ T. J. Reber et al., preprint arXiv:1508.06252.
¹⁴ S. H. Hong et al., Phys. Rev. Lett. **113**, 057001 (2014).
¹⁵ E. Abrahams and C. Varma, Proc. Natl. Acad. Sci. U.S.A. **97**, 5714 (2000).
¹⁶ P. A. Lee, N. Nagaosa, and X.-G. Wen, Rev. Mod. Phys. **78**, 17 (2006).
¹⁷ F. Herman and R. Hlubina, in preparation.
¹⁸ J. M. Bok et al., Sci. Adv. **2**, e1501329 (2016).
¹⁹ T. Bzdušek and R. Hlubina, Philos. Mag. **95**, 609 (2015).
²⁰ A.A. Galkin, A.I. D'yachenko and V.M. Svistunov, Sov. Phys. JETP **39**, 1115 (1974).